INTRODUCTION: Conceptual introduction, problem description

Introduction

Recirculating flows are commonly observed in several engineering applications, ranging from industrial processes to irrigation canals. They are often a result of a sudden change in the geometry of channels or pipes through which the fluid flows, such as orifices, baffles, sloping walls, etc. While also possible in compressible flows, recirculating flows are often observed in incompressible flows. Such flows have two key features: an upstream response to the change in geometry in the flow, and the development of negative gauge pressures and resultant recirculating flows.

In classical fluid mechanics, recirculating flows are often modeled through empirical coefficients that take into account the loss in energy or head. For example, the Bernoulli Equation for a sudden expansion along a streamline in a pipe flow is often written as (*1*):

$$\frac{p_1}{\rho g} + \frac{v_1^2}{2} + z_1 = \frac{p_2}{\rho g} + \frac{v_2^2}{2} + z_2 + \frac{k(v_1^2 - v_2^2)}{2} \qquad (1)$$

Where the first three terms on either side of equation (1) represent pressure, kinetic and potential energy heads, and the last term follows from the Borda-Carnot Equation with *k* being an empirical loss coefficient. Equations of a similar form have been derived for many other flow geometries as well. However, all of these are for regular geometries that cannot readily be extrapolated to more complex geometries or cases with different boundary conditions. In that case, when regular laboratory testing is difficult to perform, Computational Fluid Dynamics (CFD) may be employed for rapid solutions, such as in references (*2*,*3*,*4*).

However, CFD solutions should be used carefully so as to weed out grossly incorrect solutions and avoid the 'garbage-in-garbage-out' phenomenon that is all too often seen in the area. A common approach for this is to apply CFD to simple geometries for which experimental or even analytical solutions have been derived, and to compare the solutions. A CFD program thus validated, can be used with some degree of confidence for more complicated problems whose solutions are not readily available. Therefore, in this report for the ME 498 Tools of Computational Mechanics (CF1) class, two commonly-observed and well-researched geometries are modeled using a CFD solver, ANSYS FLUENT. Both the behavior of the numerical solution as well as results of the primitive variables are discussed. While the results are not validated, the solution if verified through a grid convergence test.

Problem Description

In this study, two flow geometries from a list of six possible ones were chosen for simulation. These are:

(a) Planar sudden expansion in a pipe without taper

(b) Flow over a baffle placed in a pipe

A schematic diagram of the flow geometries is shown in Figure 1. It was assumed that H = 1 m.

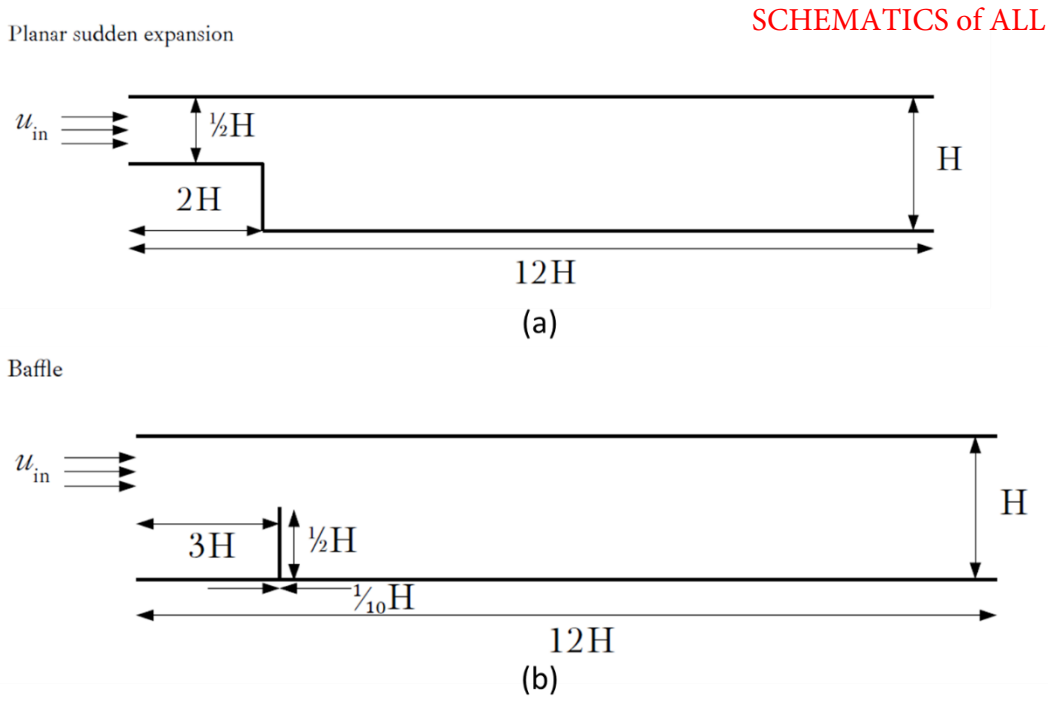

Figure 1: Flow geometries under consideration: (a) Planar sudden expansion and (b) flow over a baffle. Diagrams taken from the problem statement for ME 498 provided by Dr. Neil Davis.

For this study, flow physics were held constant (as discussed in a later section) while the grid was refined to ensure mesh convergence. The element size was subsequently set at 0.1H, 0.05H, and 0.025H in three stages. To obtain this, two mesh controls were added in the pre-processor:

(a) Edge sizing corresponding to the desired element size was applied to all the edges

(b) Face meshing was applied to the 2D flow domain

A diagram showing the final mesh is shown in Figure 2 for the planar expansion case and in Figure 3 for the baffle case. Important mesh statistics for each case are shown in Table 1, from which it can be concluded that the mesh is of very high quality.

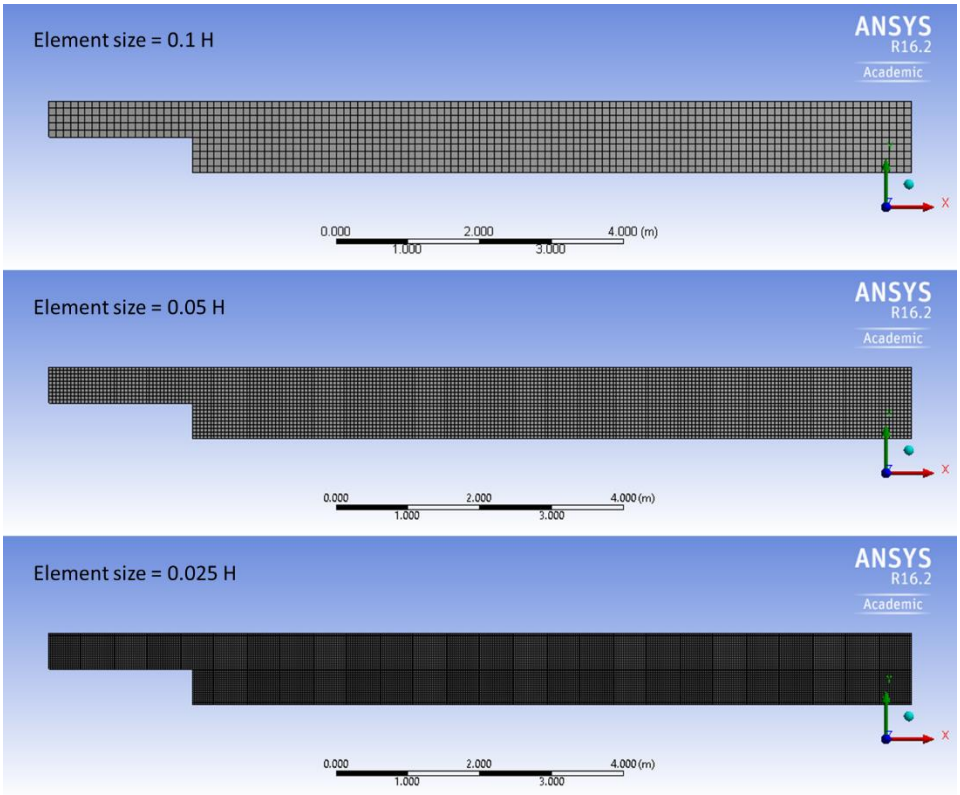

Figure 2: Final meshes for the planar expansion case for elements of size 0.1H, 0.05H, and 0.025H

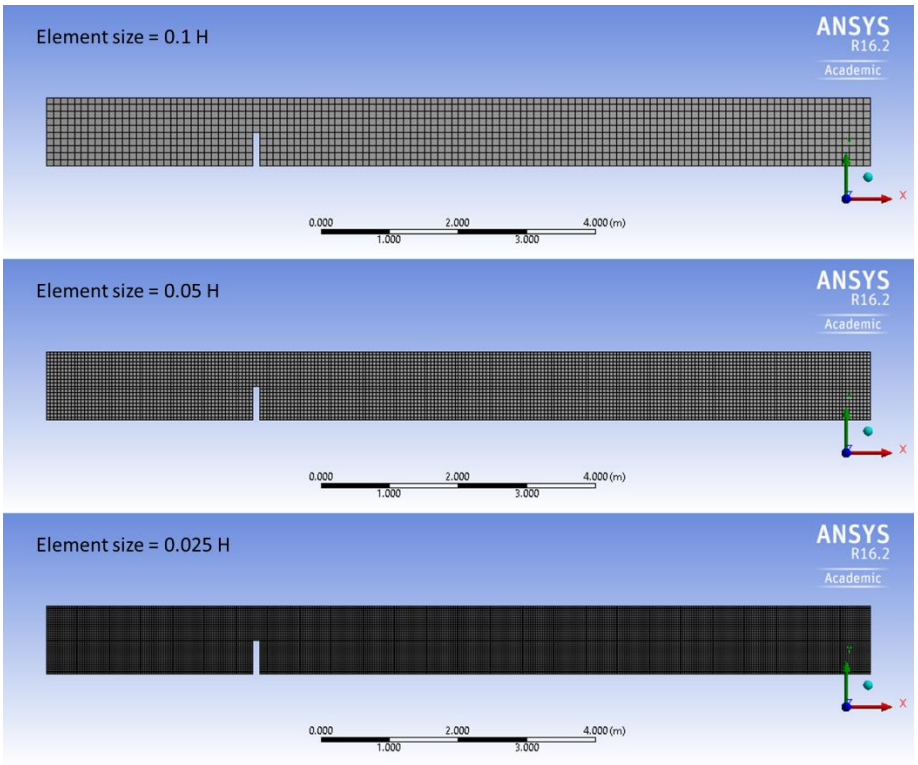

Figure 3: Final meshes for the baffle case for elements of size 0.1H, 0.05H, and 0.025H

IMAGE OF MESHED BODY WITH CORRESPONDING SETUP EXPLANATION

Table 1: Mesh statistics for each element size in the Planar Expansion and Baffle cases

	Planar Expansion			Flow over a Baffle		
	0.1H	0.05H	0.025H	0.1H	0.05H	0.025H
Number of Elements	1100	4400	17600	1195	4780	19120
Element Quality	0.99947 for 100% of elements	0.99947 for 100% of elements	0.99947 for 100% of elements	0.99947 for 100% of elements	0.99947 for 100% of elements	0.99947 for 100% of elements
Aspect Ratio	1.00000 for 100% of elements	1.00000 for 100% of elements	1.00000 for 100% of elements	1.00000 for 100% of elements	1.00000 for 100% of elements	1.00000 for 100% of elements
Skewness	Of the order of 10^{-10} for 100% of elements	Of the order of 10^{-10} for 100% of elements	Of the order of 10^{-10} for 100% of elements	Of the order of 10^{-10} for 100% of elements	Of the order of 10^{-10} for 100% of elements	Of the order of 10^{-10} for 100% of elements
Orthogonal Quality	1.00000 for 100% of elements	1.00000 for 100% of elements	1.00000 for 100% of elements	1.00000 for 100% of elements	1.00000 for 100% of elements	1.00000 for 100% of elements

Details of the Simulation

Once the pre-processing was completed and the final mesh obtained, it was read into the solver ANSYS FLUENT for each case. Double precision was used on a single-core processor with a pressure-based solver, as is common for incompressible flow. The same settings were used in each case for the grid convergence study. The fluid material was defined as a fictitious 'case fluid' as described in the next section in order to fix the Reynold's Number at 100. For this flow, laminar flow physics was suitable and the Viscous – Laminar model was activated, with all other models turned off. The SIMPLE algorithm (5) for pressure-velocity coupling was used together with the following discretization schemes:

(a) Gradient terms were discretized with a Least Squares Cell Based approach
(b) Pressure was discretized with a second order scheme
(c) Momentum was discretized with a second order upwind scheme

Three solution monitors in the form of scaled residuals were set: continuity, x-velocity, and y-velocity. The tolerance for each of these was set at 10^{-6} or 1000 maximum iterations, whichever is reached first. FLUENT allows for a Hybrid Initialization for faster convergence, which was applied before iterations were initiated.

Numerical Parameters

As outlined previously, a fictitious 'case fluid' was created to achieve Re = 100. This fluid has a density of 1 kg/m^3 and viscosity of 0.01 Pa-s. From the problem geometry, a hydraulic diameter was defined as:

$$D_H = \frac{4A}{P} \quad (2)$$

Where A is the area of the cross-section and P the wetted perimeter. For this simulation, the cross section of both the geometries (planar expansion and baffle) was assumed to be a unit square of side H = 1 m and hence, A = 1 m^2 and P = 4 m. Thus, $D_H = 4 * \frac{1}{4} = 1\ m$. SHOW CALCULATIONS

Finally, the inlet velocity (as shown in Figure 1) was assumed to be $u_{in} = 1\ m/s$, so that $Re = \frac{\rho u_{in} D_H}{\mu} = \frac{1*1*1}{0.01} = 100$. Thus, laminar flow physics was used for the solution. The grid sizes based on the value of H were 0.1 m, 0.05 m, and 0.025 m for each geometry.

The outlet was set to pressure-outlet with a gauge pressure of 0 at an operating pressure of 101325 Pa. The other boundaries were set as walls. A hybrid initialization was used to speech up convergence.

Solution

This section describes the numerical solutions obtained for each case.

Computational Times and Numerical Behavior

The number of iterations to convergence and CPU time are shown in Table 2 (obtained in FLUENT from *Reports* > *System* > *Time Usage*). As stated previously, the residuals were set to a tolerance of 10^{-6} for each variable, or a maximum of 1000 iterations, whichever is achieved first. The residuals for the planar expansion case are plotted against the number of iterations in Figure 4 and for the baffle case in Figure 5.

Table 2: Iterations to convergence and CPU user time for each case

	Planar Expansion			Flow over a Baffle		
	0.1H	0.05H	0.025H	0.1H	0.05H	0.025H
Iterations to convergence	138	334	890	296	606	1000 (max)
CPU User Time (seconds)	4.71875	13.4844	92.9531	8.48438	23.375	114.156

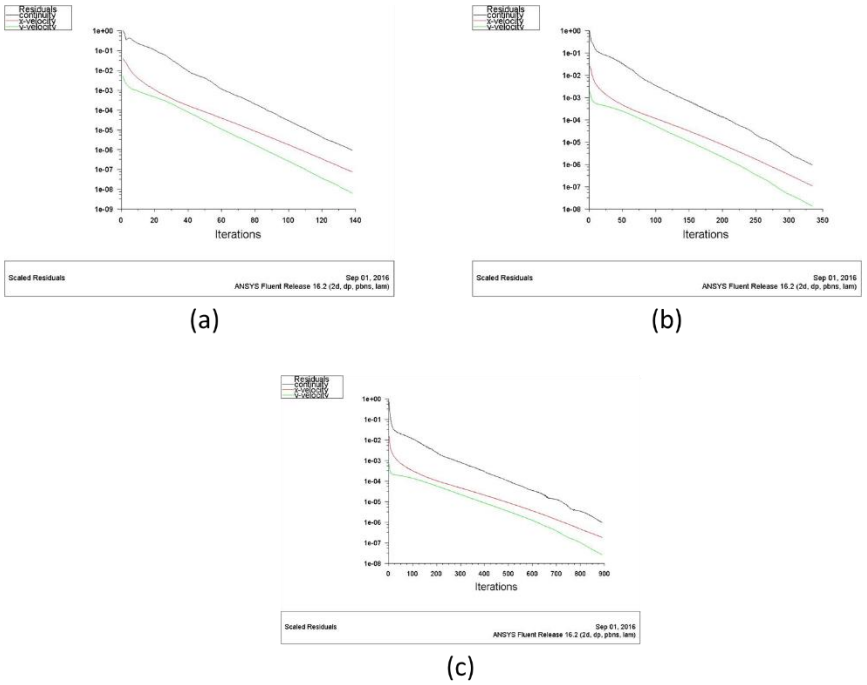

Figure 4: Residuals for the planar expansion case for grid size of (a) 0.1H (b) 0.05H and (c) 0.025H

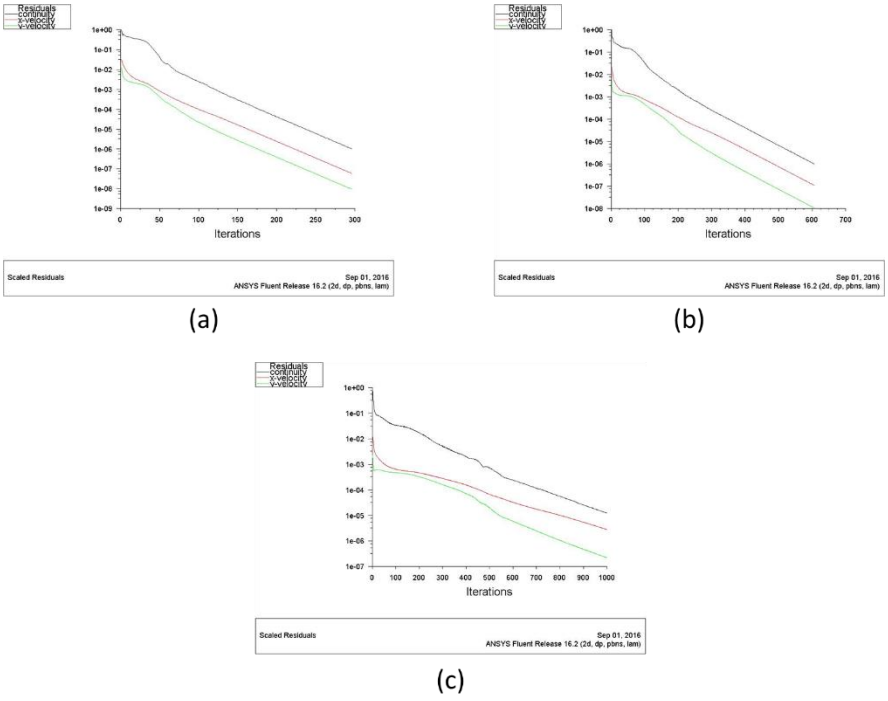

Figure 5: Residuals for the baffle case for grid size of (a) 0.1H (b) 0.05H and (c) 0.025H

For the planar expansion case shown in Figure 4, the convergence rate is more or less constant for all three grids. Convergence was reached before the maximum number of iterations (1000), with x- and y-velocities

converging to tolerance well before the continuity condition, as is typically observed. Overall, good convergence was obtained for this case.

DISCUSS CONVERGENCE FOR VARYING CRITERIA : MESH, etc

For the case of flow over a baffle, convergence was more difficult as compared to the planar expansion case with corresponding element size. Initially (about the first 100 iterations), there is some oscillatory behavior observed particularly for continuity, and after that there is more rapid convergence, although slower than the planar expansion case. In particular, the finest mesh for the baffle case does not fully converge at 1000 iterations, with the velocities reaching a residual of below 10^{-6} but continuity remaining on the order of 10^{-5}. This indicates that there is some complicated physics that is difficult to resolve for the flow over a baffle, as discussed in the next section.

EXPLANATION OF FLOW PHYSICS

Flow Physics

With the numerical solution at hand, the flow physics can be analyzed in a post-processor, CFD-Post in this case. First, a quick look at the pressure contours serves as a useful guide of where there is some significant physics underway for further analysis. The pressure contours for planar expansion and baffle cases are shown in Figure 6 and Figure 7 respectively.

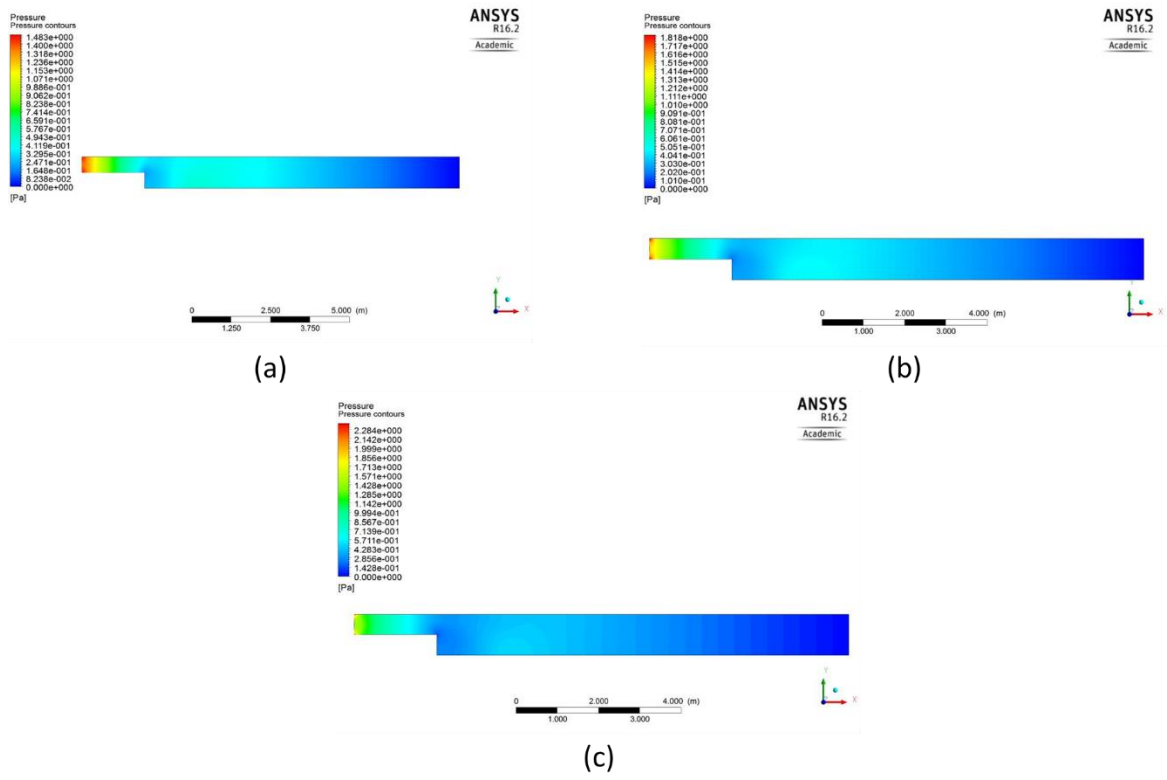

Figure 6: Pressure contours for the planar expansion case for grid size of (a) 0.1H (b) 0.05H and (c) 0.025H

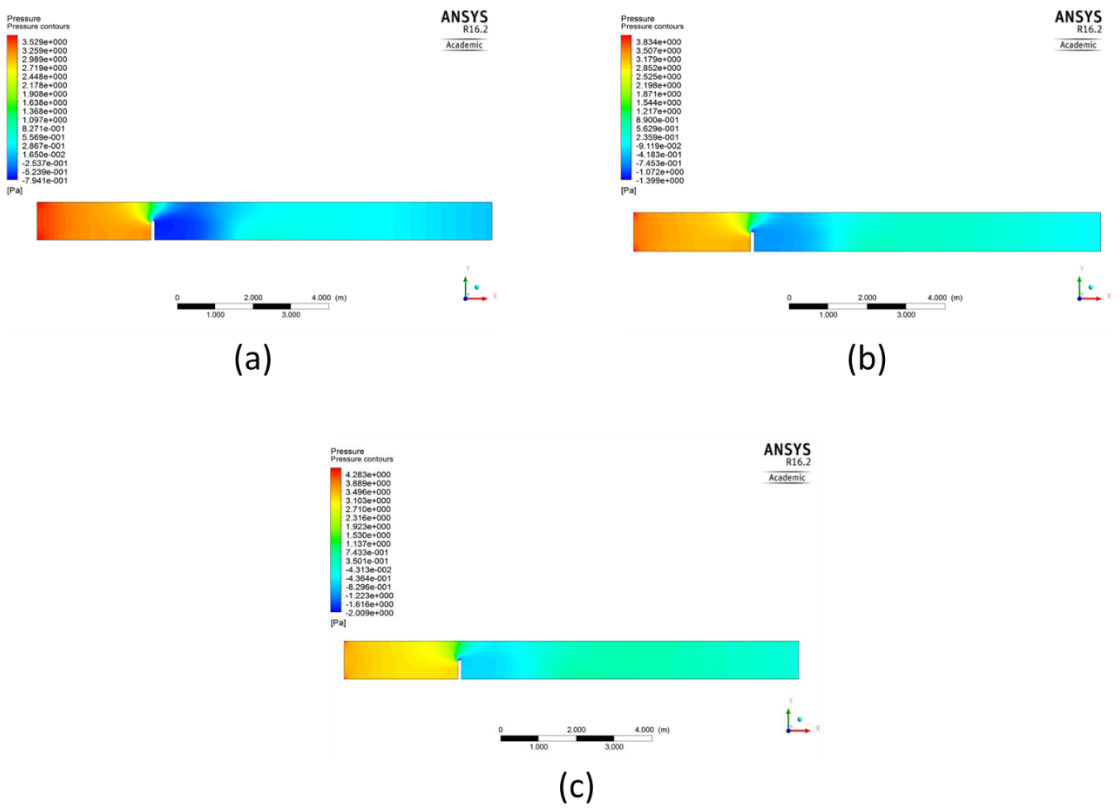

Figure 7: Pressure contours for the baffle case for grid size of (a) 0.1H (b) 0.05H and (c) 0.025H

For the planar expansion case, it can be seen that while all three meshes give similar results, the finer mesh appears to capture some localized areas of higher pressure. However, of primary interest is the pressure field near the expansion, and all three meshes indicate the development of localized low pressure areas around the expansion, indicating possible flow separation. This will be further examined through streamlines later.

OBSERVATION OF RESULTS

For the baffle case, a sudden change in pressure is observed just before and after the baffle, and it is clear that using a finer mesh leads to somewhat different solutions with decreasing size of elements. In particular, the finest mesh of element size 0.025 m leads to some large and small values of pressure being observed, which makes a localized, rapidly-changing solution difficult to capture. After the baffle, a zone of negative pressure is developed, as expected from the flow physics, leading to recirculating flow and flow separation as observed by the streamlines in the next paragraph.

The streamlines can be observed by seeding the post-processor at a particular location. In this case, two locations are possible:

(a) **At the inlet:** While this is the most obvious, it fails to capture the recirculating flow. However, it does show the upstream effect of a change in geometry on the flow.

(b) **Just after the expansion or baffle:** This approach is useful to observe the recirculating flow, but not the rest of the flow.

Streamlines are plotted for both locations (a) and (b) in order to obtain a complete picture of the flow. Figure 8 shows the streamlines for the planar expansion case while Figure 9 shows them for the baffle case.

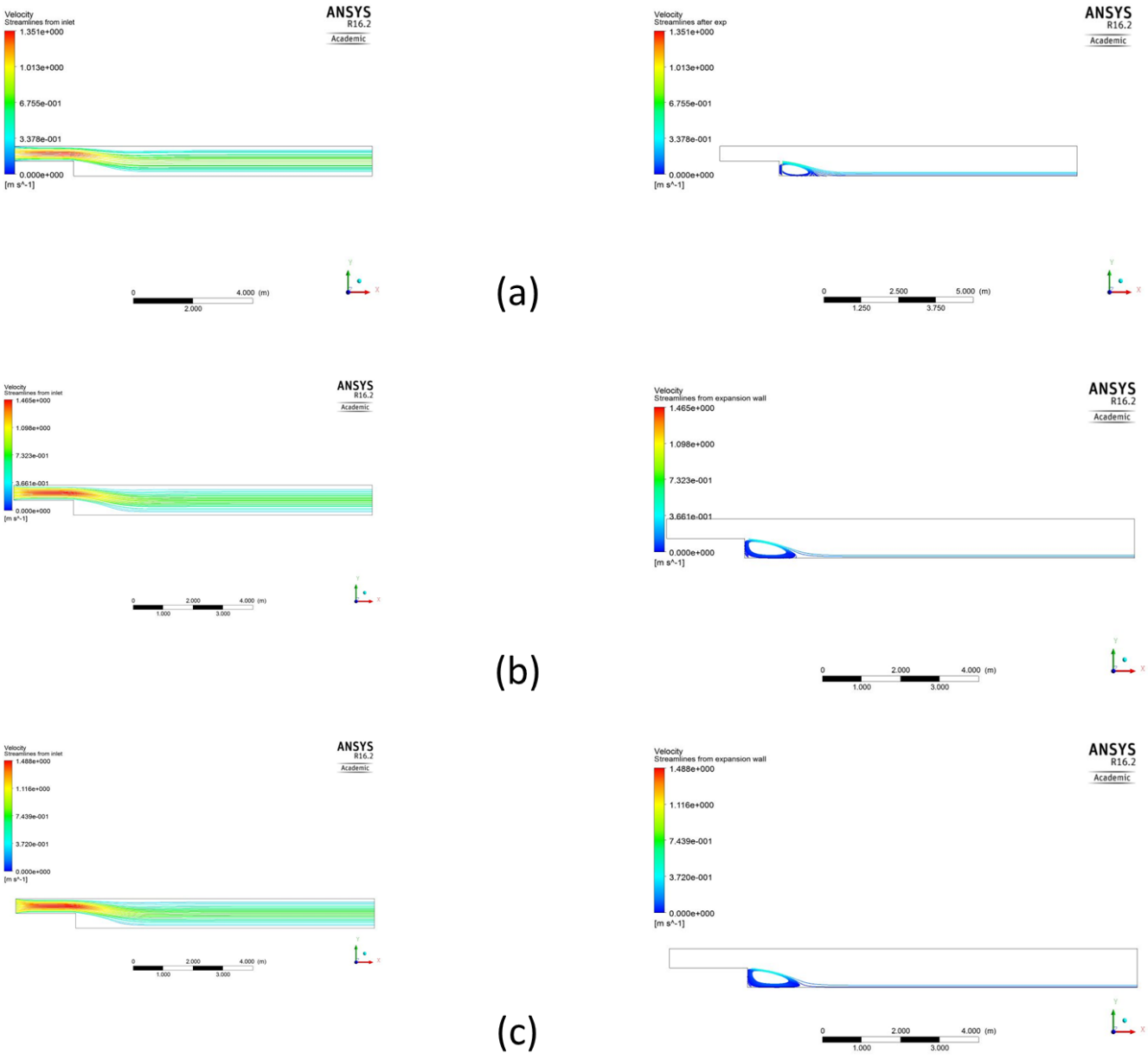

Figure 8: Streamlines for the planar expansion case for grid size of (a) 0.1H (b) 0.05H and (c) 0.025H. Diagrams on the left show streamlines from the inlet, while those on the right show them just after the expansion.

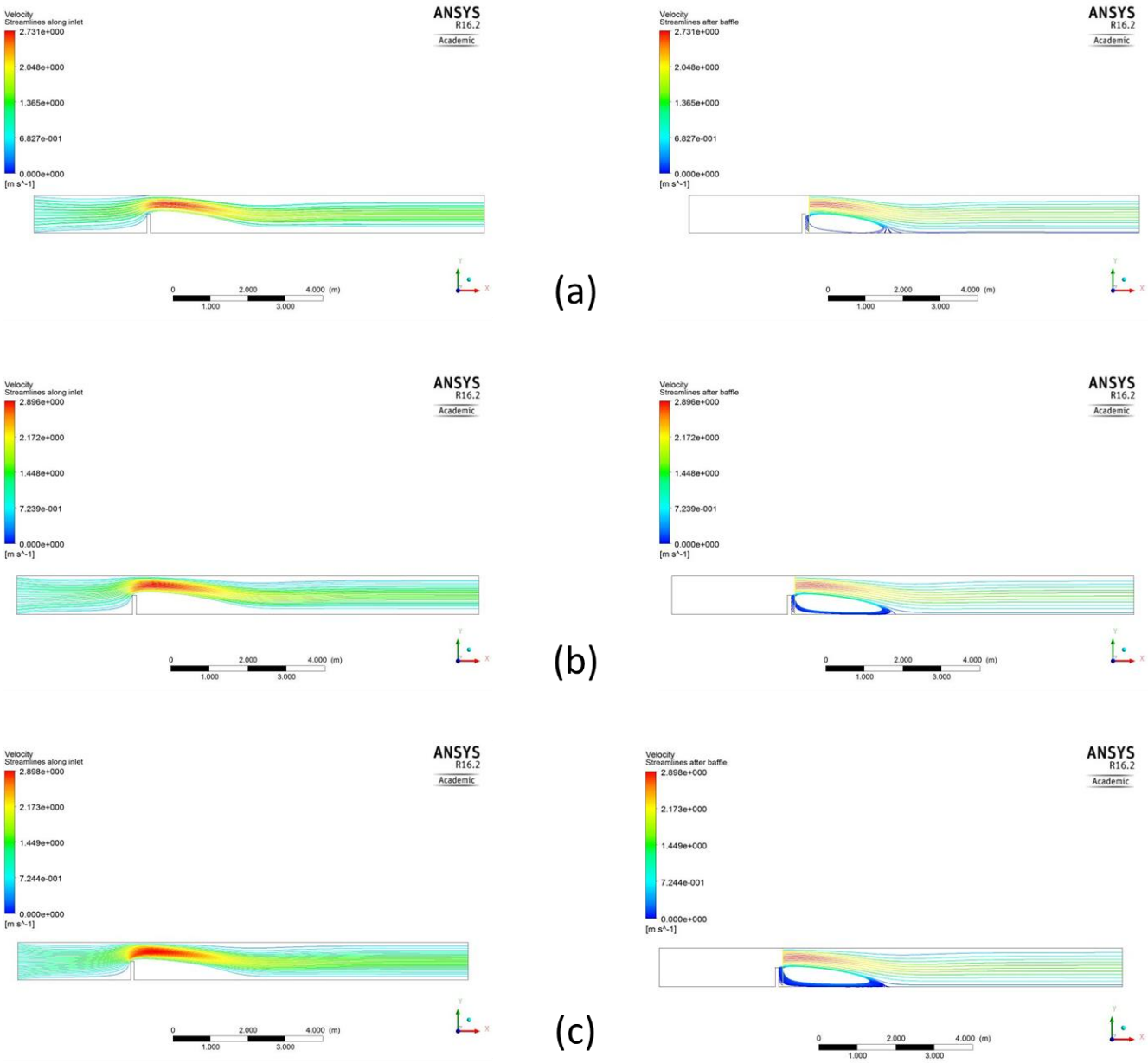

Figure 9: Streamlines for the baffle case for grid size of (a) 0.1H (b) 0.05H and (c) 0.025H. Diagrams on the left show streamlines from the inlet, while those on the right show them just after the expansion.

For both cases, the streamlines clearly capture the recirculation predicted from the pressure contours. Moreover, upstream changes to the flow can also be seen clearly in the streamlines from the inlet. Thus, the numerical CFD analysis on ANSYS FLUENT is able to resolve the flow, and the mesh refinement study appears to lead to a converging flow field.

As a final check on mesh convergence, the pressure along the wall can be plotted and compared, as shown in Figure 10 for the planar expansion case and Figure 11 for the baffle case.

PLOTS FROM OBSERVATIONS

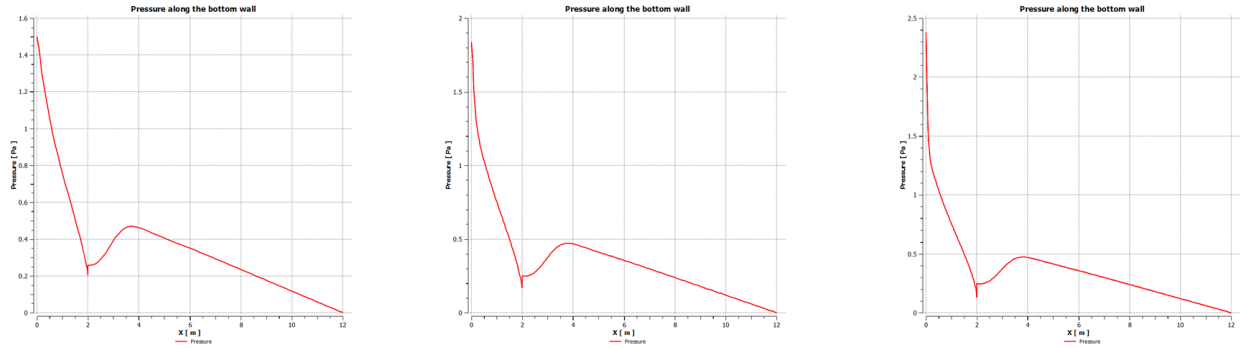

Figure 10: Pressure along the bottom wall for the planar expansion case for grid size of (a) 0.1H (b) 0.05H and (c) 0.025H.

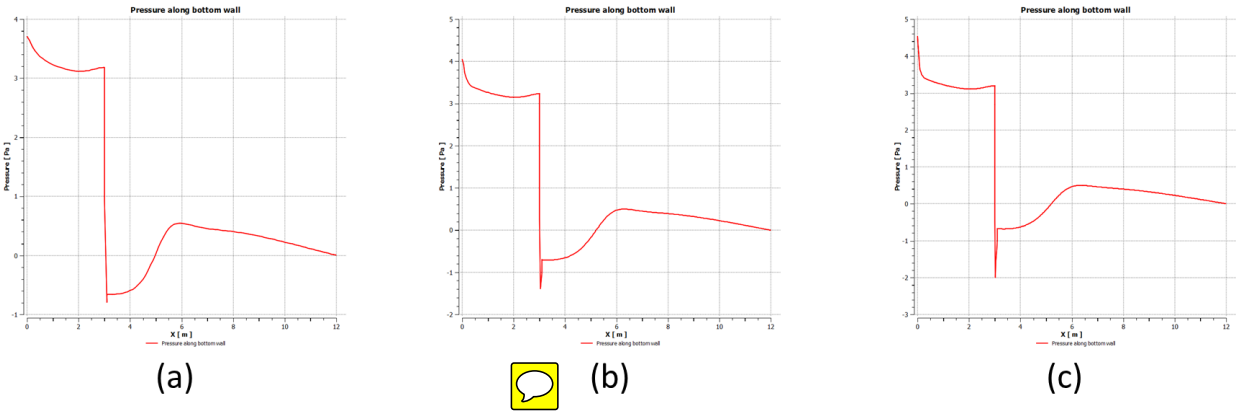

Figure 11: Pressure along the bottom wall for the baffle case for grid size of (a) 0.1H (b) 0.05H and (c) 0.025H.

In this case, mesh convergence can be clearly quantified. For the planar expansion case, the changes in inlet pressure as a result of the upstream propagation of the disturbance (i.e., the expansion) can be observed as an increasing pressure with mesh refinement. Next, the effect of the recirculating flow on the downstream pressure can also be observed. There is a sudden decrease in pressure after the expansion, which then rises again to a maximum before falling to the boundary value of zero-gauge pressure. While all the three meshes more or less agree on the position of the local maximum after the expansion, the value steadily converges to about 0.5 Pa with refinement. The sharp discontinuity or 'kink' observed at x = 2 m is because of the sudden change in geometry and is non-physical in nature. Further refinement would be necessary to obtain a smooth curve there.

INFERENCE/ EXPLANATION FLOW PHYSICS FROM OBSERVATIONS.
EITHER STANDALONE OR WITH VALIDATIONS

For the baffle case too, the upstream propagation of the disturbance (the baffle) is observed through increasing pressure at the inlet with refinement of the mesh. Downstream though, the coarse mesh (element size 0.1H) does not agree with the finer meshes in terms of the location of the downstream pressure maxima, although it does agree on the corresponding value to a large extent. However, the pressure minimum does not seem to converge with these three meshes. Thus, mesh refinement is important in this case due to the

more complex physics involved. Finally, in this case as well, a non-physical discontinuity is observed at x = 3 m because of the baffle, which can only be resolved by further refinement.

Conclusion

VALIDATIONS/CONCLUSIONS

In this study, two types of geometries, both for sudden changes, were examined for laminar flow behavior at Re = 100, with a mesh convergence study being conducted to verify the results. The results indicated that the CFD solver, ANSYS FLUENT, was able to capture expected flow physics well, although further refinement is necessary for convergence of results. In particular, the solver was able to resolve two important flow characteristics: the upstream propagation of the disturbance, and recirculation and flow separation as a result of development of low or negative gauge pressure.

In future studies, further mesh refinement, particular around the change in geometry, is recommended for better resolution of the flow.

References

REFERENCES

1. Munson; Rothmayer; Okiishi; Huebsch. *Fundamentals of Fluid Mechanics,* 7th ed.; Wiley, 2012.
2. Cheng, M.; Hung, K. C. Vortex structure of steady flow in a rectangular cavity. *Computers & Fluids* **2006,** *35,* 1046-1062.
3. Biswas, G.; Breuer, M.; Durst, F. Backward Facing Step Flows for various expansion rations at Low and Moderate Reynolds Numbers. *Journal of Fluids Engineering* **2004,** *126* (3), 362-374.
4. Xie, X.; Liu, C.; Leung, D.; Leung, M. Characteristics of air exchange in a street canyon with ground heating. *Atmospheric Environment* **2006,** *40,* 6396–6409.
5. Patankar, S. *Numerical Heat Transfer and Fluid Flow,* 1st ed.; CRC Press, 1980.